REPORT DOCUMENTATION PAGE

Form Approved
OMB No. 0704-0188

1. REPORT DATE (DD-MM-YYYY)	2. REPORT TYPE	3. DATES COVERED (From - To)
17-11-2010	Journal Article	

4. TITLE AND SUBTITLE

Video and field observations of wave attenuation in a muddy surf zone

5a. CONTRACT NUMBER

5b. GRANT NUMBER

N000173-05-1-g26

5c. PROGRAM ELEMENT NUMBER

6. AUTHOR(S)

P.S. Pereira, L.J. Calliari, R. Holman, K.T. Holland, R.M.C. Guedes, C.K. Amorin, P.G. Cavalcanti

5d. PROJECT NUMBER

5e. TASK NUMBER

5f. WORK UNIT NUMBER

74-9474-00

7. PERFORMING ORGANIZATION NAME(S) AND ADDRESS(ES)

Naval Research Laboratory
Marine Geoacoustics Division
Stennis Space Center, MS 39529

8. PERFORMING ORGANIZATION REPORT NUMBER

NRL/JA/7430-10-5

9. SPONSORING/MONITORING AGENCY NAME(S) AND ADDRESS(ES)

Office of Naval Research
800 North Quincy Street
Arlington VA 22217-5000

10. SPONSOR/MONITOR'S ACRONYM(S)

ONR

11. SPONSOR/MONITOR'S REPORT NUMBER(S)

12. DISTRIBUTION/AVAILABILITY STATEMENT

Approved for public release; distribution is unlimited

13. SUPPLEMENTARY NOTES

14. ABSTRACT

Besides the different scales within which coastal processes manifest their energy, the majority of the world's coastal regions exhibit forms of sediment heterogeneity that are physically significant. One example of a heterogeneous environment is Cassino beach, located at the southernmost part of Brazil, a fine-grain-sized sandy beach where fluid mud sporadically is transported to the nearshore and eventually onto the beach. At this site in 2005, as part of a field experiment, a video system was installed. Three years after the installation, a large mud transgression event took place in February 2008 and had 5 km of extension. In this context, the goal of the present work is to characterize the mud deposition pattern across the surf zone, describing the consequences of mud on nearshore dynamics using remote sensing techniques, beach profiles and suspended matter concentration. The surveyed beach profiles registered the deposition of fluid mud at the inner surf zone with concentrations up to 12 mg/l. The material was deposited close to the shoreline and had a cross-shore width of 100 m during the first deposition day occupying the entire water column. From surf zone time series of pixel intensity, it was possible to detect the attenuation of the surface wave spectra due to the

15. SUBJECT TERMS

wave attenuation, mud transgressed beach, remote sensing, double layer formation

16. SECURITY CLASSIFICATION OF:			17. LIMITATION OF ABSTRACT	18. NUMBER OF PAGES	19a. NAME OF RESPONSIBLE PERSON
a. REPORT	b. ABSTRACT	c. THIS PAGE			Todd Holland
Unclassified	Unclassified	Unclassified	UU	13	19b. TELEPHONE NUMBER (Include area code) 228-688-5320

Standard Form 298 (Rev. 8/98)
Prescribed by ANSI Std. Z39.18

Video and field observations of wave attenuation in a muddy surf zone

P.S. Pereira [a,*], L.J. Calliari [a], R. Holman [b], K.T. Holland [c], R.M.C. Guedes [d], C.K. Amorin [a], P.G. Cavalcanti [e]

[a] Laboratory of Geological Oceanography, Institute of Oceanography, Federal University of Rio Grande, Av. Itália, km 8, C.P. 474, Rio Grande, RS 96201-900, Brazil
[b] College of Oceanic and Atmospheric Sciences, Oregon State University, Corvallis, OR, United States
[c] Naval Research Laboratory, Stennis Space Center, MS, United States
[d] University of Waikato, Department of Earth and Ocean Sciences, Hamilton, New Zealand
[e] Institute of Informatics, Federal University of Rio Grande do Sul, Porto Alegre, RS, Brazil

ARTICLE INFO

ABSTRACT

Besides the different scales within which coastal processes manifest their energy, the majority of the world's coastal regions exhibit forms of sediment heterogeneity that are physically significant. One example of a heterogeneous environment is Cassino beach, located at the southernmost part of Brazil, a fine-grain-sized sandy beach where fluid mud sporadically is transported to the nearshore and eventually onto the beach. At this site in 2005, as part of a field experiment, a video system was installed. Three years after the installation, a large mud transgression event took place in February 2008 and had 5 km of extension. In this context, the goal of the present work is to characterize the mud deposition pattern across the surf zone, describing the consequences of mud on nearshore dynamics using remote sensing techniques, beach profiles and suspended matter concentration. The surveyed beach profiles registered the deposition of fluid mud at the inner surf zone with concentrations up to 12 mg/l. The material was deposited close to the shoreline and had a cross-shore width of 100 m during the first deposition day occupying the entire water column. From surf zone time series of pixel intensity, it was possible to detect the attenuation of the surface wave spectra due to the presence of fluid mud. The combination of video techniques and field data allowed one to follow the formation of a double-layer system, where fluid mud overlays the sandy bottom. The video-based system at Cassino demonstrated that remote detection of fluid mud and quantification of its effect on the nearshore dynamics is feasible. The combination of beach profiles, measurements of suspended matter concentration and intensity timestacks allowed the analysis of the short-term evolution of the mud depositional processes.
© 2010 Elsevier B.V. All rights reserved.

1. Introduction

Nearshore processes involve many spatial and temporal scales, from a few millimeters to hundreds of kilometers, from seconds to decades, or even centuries. Besides the different scales within which coastal processes manifest their energy, it is a fact that the majority of the world's coastal regions (between 60% and 80%) exhibit forms of sediment heterogeneity that are physically significant in terms of estimation of bottom friction and wave attenuation (Holland and Elmore, 2008). These types include gravel–sand coasts, sorted bed-form fields, sand-ridge fields, cheniers, mud transgressed beaches, mixed tidal flats and graded foreshores (Holland and Elmore, 2008).

A heterogeneous sediment type that calls for attention regarding its effects on coastal process is the mud transgressed beaches. Normally, beaches are coastal environments composed of sand, gravel and cobbles dominated and formed by wave action. However, at a few places around the globe, the sand bottom and beach are episodically overlain by a relatively thick mud layer, as documented on beaches located north of the Amazon river (Augustinus et al., 1989; Wells and Coleman, 1977; Winterwerp et al., 2007); at the southwestern coast of India (Mathew et al., 1995); and also on the southern coast of Brazil (Calliari et al., 2001, 2007).

When these transgression events occur, a sharp horizontal and vertical boundary exists between the two sediment types, mud and sand. Theoretical studies and field observations have shown that when the mud is at a fluid state over the bottom, the waves are rapidly attenuated while propagating over it, resulting in a strong decay of wave height within a few wavelengths (Gade, 1958; Mathew et al., 1995).

Surveying the abovementioned variety of scales and sediment heterogeneities has never been an easy task, challenging scientists all over the globe to develop tools that can continuously cover all scales. A variety of tools based on acoustic and visual band optic signals have become available, often providing startling insights (Holman, 1995). In this context, remote sensing techniques offer an attractive tool for the measurement of the different scales involved in nearshore processes.

Since 1985 video techniques have been used worldwide to survey the nearshore environment, which is replete with optical signatures

* Corresponding author. Federal University of Pernambuco, Oceanography Department, Laboratory of Geological Oceanography, Av. Arquitetura, s/n, Cidade Universitária, Recife, PE, Brazil, Zip: 50.740-550. Tel.: +55 81 2126 7225.
E-mail address: praia@log.furg.br (P.S. Pereira).

mean significant height of 1.5 m from S/SE quadrant with a period ranging from 6 to 8 s, which corresponds to sea conditions. Storm surges are responsible for the highest water level oscillations over the beach and are mainly caused by the presence of a low pressure system on the adjacent ocean and a high pressure system in the continent. According to Calliari et al. (1998), the surge level can reach 2 m, approximately four times the mean tidal range of 0.47 m according to Möller et al. (2001). Regarding the wind, northeasterly (NE) winds dominate throughout the year. Southwesterly (SW) winds become more important during fall and winter as frontal systems become more frequent over this area (Möller et al., 2001). Typical wind speeds are between 3 and 5 m s^{-1} (Tomazelli, 1993).

3. Data set

3.1. Video imagery

The Argus camera network consists of video cameras installed over high land areas or in towers at many beach locations around the globe (Holman and Stanley, 2007). The system routinely captures images from the beach and surf zone during the first 10 min of each daylight hours processing, storing and transmitting them to selected laboratories of coastal studies. At Cassino, the station is composed of four cameras installed at the top of a 14 m tower (see Fig. 1 for its location).

There are three main Argus products: a single snapshot, a 10-minute time-exposure and a 10-minute variance image (Holman and Stanley, 2007). The snapshot is a single video frame collected at the beginning of each hour. The time-exposure image, or *timex*, is a 10-minute average of all video frames collected during this time interval and, the last type, the variance image, represents the standard deviation of all the same frames used to make the timex. Each image can be rectified and merged to a single plane view image. At Cassino, the rectified image is set to have a grid of 1.0×1.0 m. The rectification process (Fig. 2) is a transformation of all two-dimensional image pixel coordinates to real world three dimension coordinates x, y, and z (Holland et al., 1997).

Another product is the pixel timestack, which is a time-series of optical intensity from an array of pixels at any desired location in the image. Pixel time-series, or pixel timestacks, can be used to estimate wave spectra because of variations in sea surface slope due to wave propagation across the array. Usually, the landward face of the wave is darker than the trough, causing intensity variations. Instead of recording full video frames for 17 min, this product is designed to register the time variation of pixel intensity at certain locations with an acquisition rate of 2 Hz (Holman and Stanley, 2007). Such an array was developed to match in situ instrumentation arrays and can be thought of as pixel instrument arrays, used to make estimations of wave periods and currents, for example.

For the present work, a cross-shore pixel array (Fig. 2) was used to calculate frequency–space plots that can be used to identify areas where the wave signal is best observed. The frequency–space plot spectra were calculated using 42 degrees of freedom and a bandwidth of 0.0205 s^{-1} at each cross-shore position.

At Cassino, the pixel array was designed to cover the full extent of the surf zone and a part of the dry beach. Prior to the collection, a cross-shore array was planned to be perpendicular to the shoreline in accordance with the local coordinate system, in which x, y and z represent the cross-shore, the longshore and vertical locations, respectively. Using the known geometry of the image, the list of sampling locations (x_i, y_i and z_i) was converted to a corresponding list of pixel coordinates (U_i, V_i) (Holland et al., 1997).

In addition to the Argus station, a set of two video cameras, was installed on the roof of the Villa Moura Hotel, 3 km north of the Argus cameras (Fig. 1). Similar to the Argus, the cameras at the Villa Moura Hotel collected a 10-minute video every hour that was then post-processed to produce snapshot, time exposure and variance images.

3.2. Beach profiles

Nearshore beach profiles and bathymetry were measured within three days of mud deposition (February 13, 14 and 20, 2008) using a total station and an optical prism. Since the beginning of the 2007/
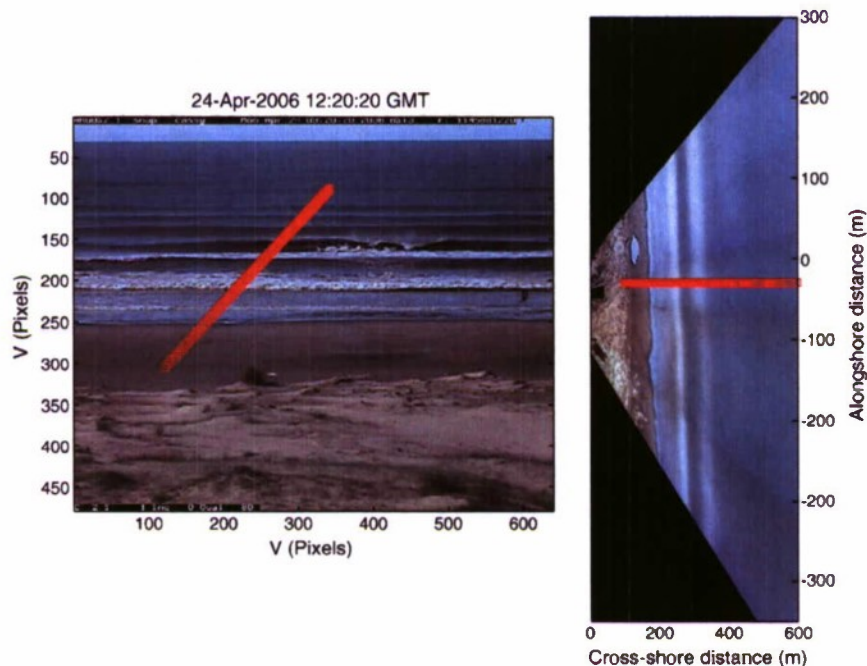

Fig. 2. Example of a single snapshot from camera two with the U and V positions of the cross-shore pixel array marked as squares (left image). Merged time exposure with rectified image of the four cameras with real world location (y = − 30) of the cross-shore pixel array on camera two (right image).
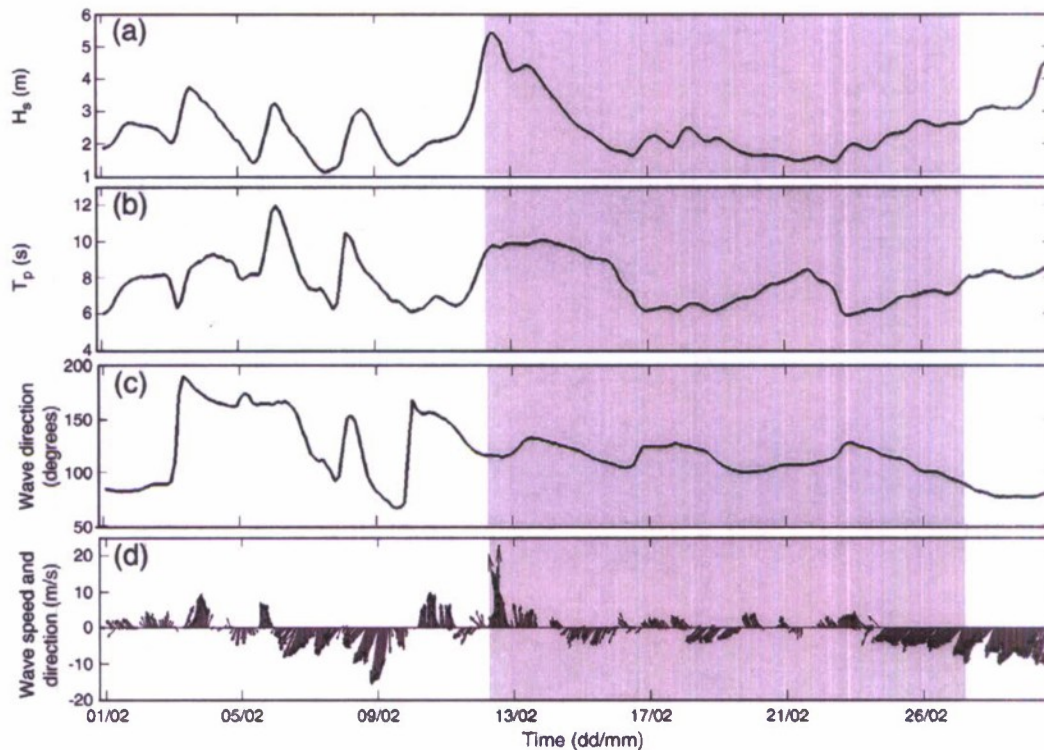
Fig. 3. (a) Significant wave height, (b) peak period, (c) peak direction and (d) wind speed and direction. The waves were estimated using the Wave Watch third generation model implemented by Melo et al. (2008). The wind data were collected at the pilot's station (see Fig. 1); negative values indicates northern quadrants wind and positive values, southern. The shaded area represents the period during which the surf zone was visually under influence of the mud deposit.

2008 summer, a series of beach profiles was obtained near the Villa Moura Hotel as part of a beach safety program implemented by the Laboratory of Geological Oceanography (LOG) of the Federal University of Rio Grande (FURG). The profiles had a mean sampling interval of two days; one of these profiles will be here used to describe the mud deposition on February 1. For both profiles, at the Villa Moura and at the Argus station, the elevation is relative to the Brazilian geodesic vertical datum (BGVD).

All transects followed the same orientation transverse to the shoreline. They extended to a maximum depth of 2.2 m, limited by the survey rod height. The profiles were interpolated to a regular spacing of 1 m along the cross-shore direction, beginning at a benchmark placed over the foredunes, in front of the Argus video cameras. This bench mark is also the local coordinate system origin (0, 0) which is the same used as in the Argus coordinate system. The profile line was located just 30 m north from the cross-shore stack line described in the previous section. During the survey of the last profile, February 20, a bathymetric profile was sampled using a boat equipped with a 200 kHz echosounder. However, due to technical problems, it was not possible to use the boat GPS data, but since one of the navigation lines was known to be at $y = 0$ m, it was possible to match and rescale some morphologic features allowing the use of at least a part of the echosounder data to measure the bathymetry.

3.3. Wave and wind data

Due to the absence of sufficiently long sampled data sets, we had to rely on numerical models to infer the wave climate offshore of Cassino beach. The results used herein were extracted from a comprehensive study carried out by Melo and his collaborators (see Melo et al., 2008 for further information). In the ongoing study, the wave generation

model Wave Watch III (WW3) is forced with NCEPs[1] reanalysis winds to reconstruct sea state conditions off the southern Brazilian coast from 1979 to 2008. In addition to the wave model data, the local wind is measured hourly at the pilot's station (Fig. 1) at the top of a tower 20 m above the ground.

3.4. Suspended matter samples

To characterize the presence of mud in the surf zone, suspended matter was collected alongshore using 1-liter plastic bottles. The samples were taken 300 m apart from each other along the beach on February 13, 14, 15 and 20 in the inner surf zone. All the samples were collected over the first trough, which separates the first bar from the beach and 0.30 m (± 0.15 m) below the water surface on a location where the mean depth is 1.1 m (± 0.25 m). The samples were first dried to determine the dry weight; the organic/inorganic content was determined based on the dry weight before and after exposition to 500 °C, which burns all the organic (carbon) content.

4. Description of 2008 mud deposition event

In February an extra-tropical cyclone formed in front of Rio Grande city, where Cassino beach is located. Wind speeds reached 22 m/s (Fig. 3d) and were mainly from the south/southeast. The cyclone generated strong winds in the deep ocean which in turn, combined with a long fetch area, generated waves that reached heights up to 5.5 m offshore of Cassino, as seen from the WW3 model data shown in Fig. 3a. On the coast, the wave height was nearly 2.5 m, as estimated

[1] NCEP/NOAA National Centers for Environmental Prediction.

by visual observations. As the cyclone moved away from the coast, the wind speed decreased as seen on February 13 (Fig. 3) but the waves kept coming in as swell.

As with other similar meteorological events that reach this area every year, this one resulted in the resuspension and transportation of mud deposits found offshore of Cassino (Calliari et al., 2007). The strong winds generated local sea waves which, combined with a high swell, can drive the fluid mud toward the coast. Calliari et al. (2009) suggest a few mechanisms to explain the occurrence of fluidized mud in the area. In the first mechanisms, waves can liquify the mud, upon which the waves are then damped by viscous dissipation within the fluid mud. The waves can also carry the fluid mud further onshore, even on to the beach. An alternative explanation is that the historical mud deposits can be eroded during extreme storms to bring large volumes of mud into suspension. Conversely, high sediment concentrations generated by flushing of the lagoon could also result in fluid mud being deposited on the shoreface, perhaps over moderately long periods of time, which can be eventually moved to the shore. On the first deposition day, February 13, surveys indicated that the area of deposition extended 5 km along the beach and had an average cross-shore extension of 100 m, from the shoreline toward the surf zone. The average mud thickness was nearly 1 m but 1.2 m at some locations.

A key element to understanding the way fluid mud reaches the shore is the Stokes drift. Wells (1983), Wells and Coleman (1977, 1981), and Wells et al. (1979) demonstrated that sinusoidal waves propagating over fluid mud bottoms could be transformed into solitary-like waves in water depths from 1 m to 5 m. The solitary-like wave formation causes a general mass transport of mud toward the beach. This mass transport would result in high water levels up on the beach face, the so called set-up (Bowen et al., 1968); however, in the present situation, fluid mud instead of water is being piled up on the beach face.

5. Data analysis and results

On the day before the mud deposition event (February 12) the surf zone looked normal, as demonstrated by collection of pixel timestacks (Fig. 4a). The timestacks shown in Fig. 4a and b were collected at specified cross-shore locations by the Argus station. The cross-shore timestack illustrates the variations in wave amplitude (or, for the video technique, pixel intensity) at each cross-shore location through time.

The white patterns at cross-shore locations 225, 277 and 367 m (Fig. 4a) denote that waves are breaking at the shoreline and over the first and second bars respectively. These patterns result in peaks in the variance intensity profiles (Fig. 4a bottom). Another pattern evident in the stacks is the presence of surface waves propagating across the surf zone, in which the dark oblique lines with low intensity values indicate the waves' face. Both patterns were visible in all stack images during this day.

On the following day (February 13) this scenario started to change (Fig. 4b), as this was the first day that the mud appeared on the beach. During all timestacks on this day, the fluid mud signal could be seen at the water surface through darker values of pixel intensity throughout the surf zone (Fig. 4b). The mud pattern on the surface is marked by a light gray pattern close to the shoreline, between 210 and 300 m, with intensity values close to 150. The mud signal made a strong contrast between the "dirty" surf zone filled with fluid mud (between x = 210 and 300 m) and the "clean", or less dirty surf zone with some fine sediment in suspension (beyond x = 300 m).

In addition to the mud signal, this image shows that wave breaking intensity (approximated by pixel brightness) is greatly reduced. The well-defined pattern of breaking waves at the shoreline and over the first and second nearshore sand bars shown by intensity maxima in the variance plot of the day before is largely destroyed. In Fig. 4b some white foam at the cross-shore location 600 m offshore barely indicates the
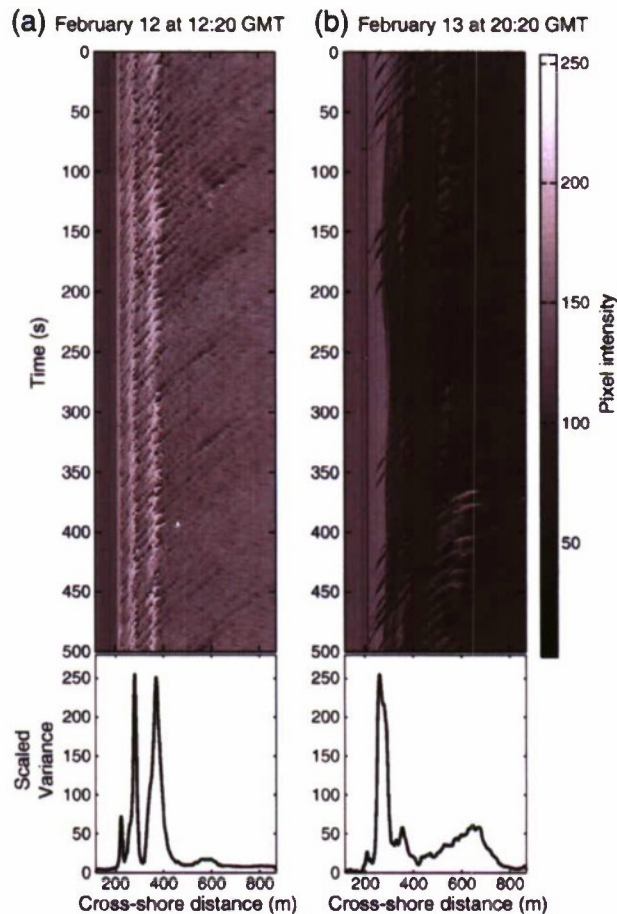

Fig. 4. Argus cross-shore intensity timestacks from (a) February 12 at 12:20 GMT and (b) February 13 at 20:20 GMT. The timestack is a collection of pixel intensity time series sampled at selected locations. The slightly curved patterns are individual waves propagating onshore. Insets give the variance structure of pixel intensity for the cross-shore transect.

presence of a third sand bar. It should be highlighted here that the absence of the white pattern is due to the amount of suspended matter in the surf-zone and this does not mean that breakers are absent. Even without a clear white foam pattern over the first bar, a variance peak continues to be perceived, probably due to the shoaling process over it.

Another way to look into the mud transgression effects on the surf zone is through frequency–space plots. A frequency–space plot showing the variability of the wave spectral density at each cross-shore location can be used to observe the wave signal across the surf zone. The spectral analysis of the stack gives the peak period of the incoming waves. As the waves are propagating from outside the surf zone toward the shoreline, the peak period is not expected to change. An exception occurs on occasions where harmonics are created due to non-linear interactions.

Fig. 5 shows a sequence of frequency–space plots during the first three days of the mud deposition event. On the day before the deposition (February 12) the spectral peak is constrained between x = 200 m and 400 m and is most clearly defined at 0.11 Hz, approximately 9 s (Fig. 5a). According to the WW3 wave model data (Fig. 3b), wave periods lower than 10 s were expected for this day. On the following day, the spectral peak has changed to 0.08 Hz which results in an increase in the peak period to approximately 12.5 s, higher than the 10 s estimated by the WW3 (Fig. 3b). As
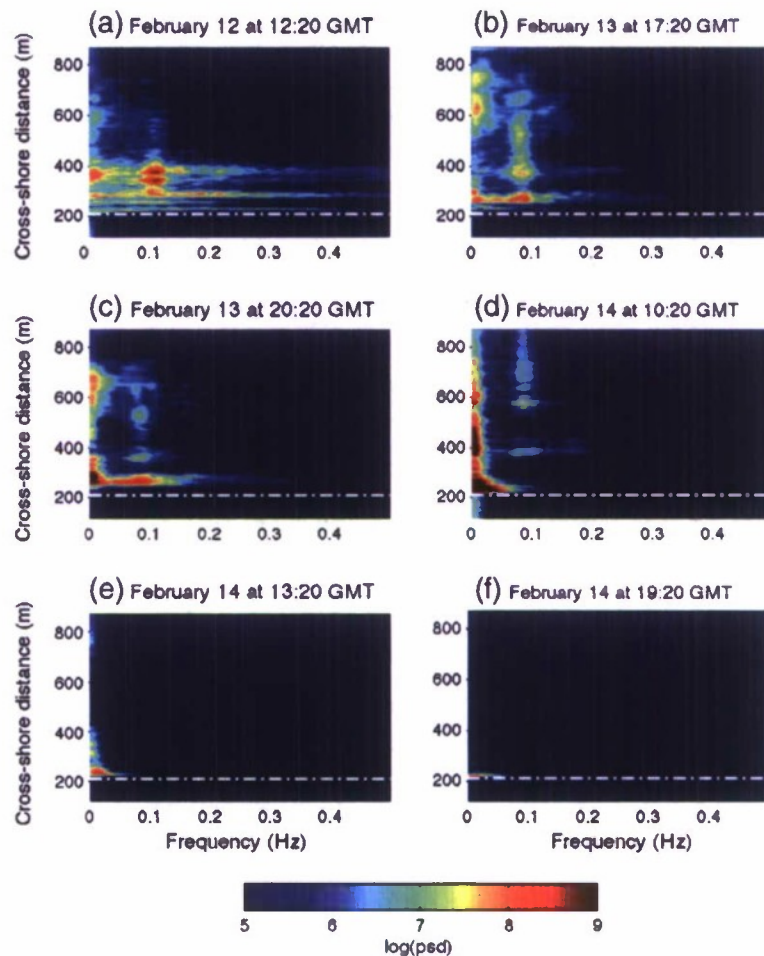
Fig. 5. Frequency–space plots of Argus intensity data at the day before the mud deposition and during the first two days of the deposition event. The dot dashed line corresponds to the shoreline location.

mentioned in Section 3, this day was characterized by a swell, which can be seen in the frequency–space plots (Fig. 5b) and the time-stacks (Fig. 4). In Fig. 4a and b this difference can be observed by comparing the dark sloping lines representing individual waves approaching the shoreline from offshore. In Fig. 4b the distance among the traces is greater than at Fig. 4a, and this information combined with the peak period estimated from Fig. 5c characterizes swell.

Besides changes in wave period, the frequency–space plot shows the signal loss of surface waves along the sequence shown in Fig. 5. If the frequency of incoming waves is selected outside the surf zone (between $x = 600$ m and 800 m) and tracked along the frequency–space plots, it is possible to see frequency modification. On the first deposition day when the waves were high and the mud was resuspended, transported and kept close to the shoreline, the incident peak period did not undergo any major changes: the spectral peak was still at the same frequency and could be found either at $x = 600$ m or between $x = 400$ m and 300 m (Fig. 5b and c). However, on February 14 this pattern started to change; from 10:20 to 19:20 GMT, there is a loss of the spectral energy across the surf zone (Fig. 5d, e and f). In Fig. 5d and e, a spectral peak still can be seen at the offshore limit of the frequency–space plot but disappears in Fig. 5f.

Fig. 6a shows the profile measured near the Villa Moura Hotel on the first deposition day, when the mud was kept close to shoreline. Due to limitations in the methodology, it was possible to survey the profile to a

depth of only 1.6 m and the distance of 410 m, which corresponded to the limit between the dense fluid mud and the normal surf zone. The fluid mud during this day was deposited in the inner surf zone, covering the first bar–trough system. Fig. 7 shows the fluid mud thickness, which reached a maximum of 1.2 m on the second deposition day (Fig. 7b) and was possible to be measured due to its high density. From Figs. 6a and 7b it can be observed that the fluid mud occupied the entire water column giving a thickness/depth ratio of 1. It is important to note that although it was not possible to survey the profile right in front of the Argus video cameras on the first day, the situation there regarding mud thickness was the same (Fig. 6a): the mud thickness/depth ratio was estimated to be closer to 1 with its offshore limit at 100 m from the shoreline.

Short elevations of the sea level, probably caused by surge and wave set-up, caused the mud to be deposited upon the beach face (Fig. 6a and b). The material deposited upon the beach face had only a few centimeters of thickness and a few meters of width. Fig. 6a and b shows that the mud profile changed its thickness and extension across the surf zone. On February 14, again, due to limitations in methodology, the profile was surveyed to a depth of 2.2 m, which almost reached the second bar crest. The maximum cross-shore distance reached on this day was 350 m, 140 m from the shoreline.

Eight days after the deposition (on February 20), the mud remained on the profile (Fig. 6c). The profile on this day was surveyed farther than the other and reached a distance of 395 m from the
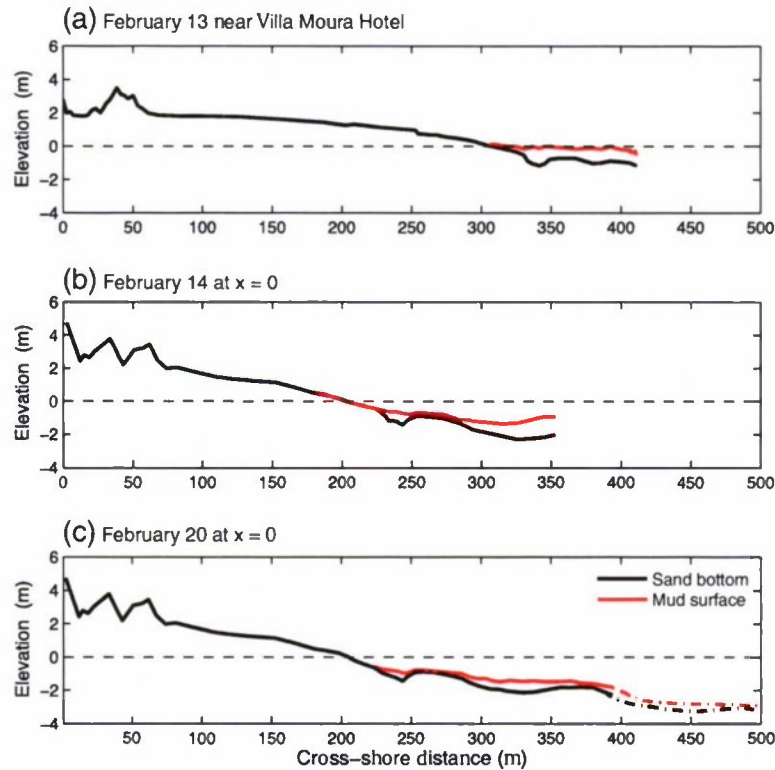
Fig. 6. Beach profiles measured on (a) February 13 near the Villa Moura Hotel (see Fig. 1 for its location) and (b) February 14 and (c) 20 at x = 0 m of the Argus coordinate system. Cross-shore distances are relative to benchmarks placed on the foredunes. The elevation is relative to the Brazilian geodesic vertical datum (BGVD). The dashed line represents the mean sea level relative to the datum. The dot and dashed lines at (c) represent the sand bottom and the mud surface measured with the echosounder.

benchmark. The echosounder data represented by dashed lines are also shown in Fig. 6c. The figure analysis shows that the mud covered the entire surf zone profile from the inner trough toward what seems to be the beginning of the third bar. Although only a little stretch of the profile was surveyed by an echosounder, the offshore limit of the mud was not found. It is believed that this limit is beyond the surf zone and might be located in the inner shoreface.

Using the profiles presented in Fig. 6a it was possible to calculate the overall volume of fluid mud deposited on the profile as 68 m^3/m. Combining the information about the mud deposition event presented in Section 3 and the calculated volume, it is possible to infer that the total volume deposited upon the beach and surf zone along the 5 km is 340,000 m^3. It should be highlighted that this number is an extrapolation and considers the same beach profile alongshore, uniform slope and shape, and an offshore mud limit of nearly 100 m, which may not be true due to limitations in the methodology used to survey the profile. However, clearly this is a significant deposition that should impact surf zone wave processes.

Fig. 8 shows the suspended matter concentrations at the inner surf zone stations along the beach during the first eight days of the deposition, where Station 3 is near the Villa Moura Hotel and Station 10 is in front of the Argus station. As seen in Fig. 8a, the first day was the day with the highest concentration of suspended matter (Station 8, 12 g/l). On this day, the fluid mud was detected in the surf zone over 5 km alongshore. The general pattern of distribution of suspended matter collected on the first day resembles a Gaussian distribution; this leads to the conclusion that the material gets concentrated over the central deposition area. Stations 1, 2 and 13 represent the edge of the deposit during the first day and display high suspended matter

concentrations. Beyond these points, there were no mud deposits in the surf zone or on the beach. This scenario changed on the next day when the mud started to migrate. The migration pattern was marked by the increase of suspended matter concentrations at the southern edge of the deposit and decrease at the northern edge, as displayed in Fig. 8a and c. This indicates a migration of 1.5 km to the south. The lowest suspended matter concentration was found on the eighth day after the mud had settled, as will be discussed in the next section.

The suspended matter collected during the deposition was examined to determine its content of organic and inorganic material and density. The organic content ranged from 21 to almost 89%; the inorganic, from 11 to 79%, the highest value of organic matter was found at station number 5, thus resulting in the lowest inorganic content. The material density ranged from 1.03 to 1.45 kg/m^3, from approximately salt water to what it is being considered here as fluid mud.

6. Discussion

The mud deposition process changed the normal surf zone behavior as demonstrated in the timestack plots (Fig. 4) and in the frequency–space plots of intensity data (Fig. 5). In Fig. 5 it is possible to observe the peak period of the surface waves that propagate across the surf-zone. Although the spectral peaks do not change in frequency, the spectral energy is attenuated across the surf-zone. This behavior, detected on February 14, is believed to be caused by a fluid mud layer on top of the natural sandy bottom, as demonstrated in Fig. 6b and c. It is important to notice that the attenuation detected is estimated by intensity data collected with a video camera, the
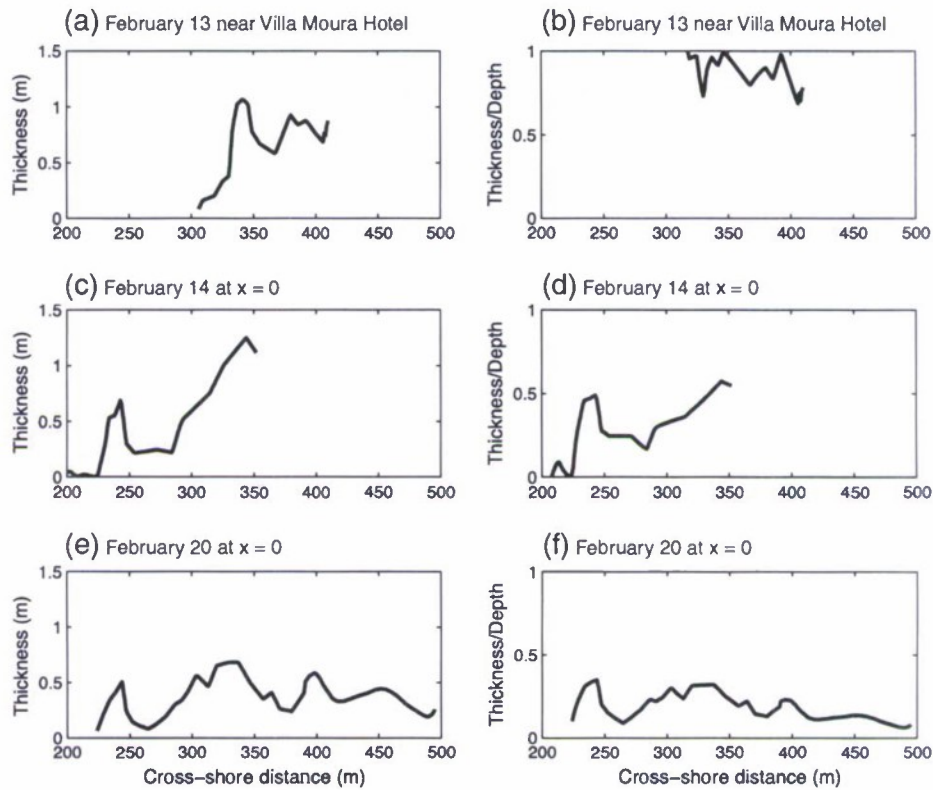
Fig. 7. Left column: fluid mud thickness for each one of the profiles presented in Fig. 6. Right column: thickness/depth ratio for each of the profiles presented in Fig. 6.

values of which oscillate according to the wave passage across a single pixel.

The described situation represents a two-layer system consisting of a water layer covering fluid mud in sharp contact with a sandy bottom. A number of physical mechanisms of wave dissipation over muddy bottoms based on different models of sediment rheology have been proposed. However, a common point among them is the requirement for the waves to be in intermediate to shallow water
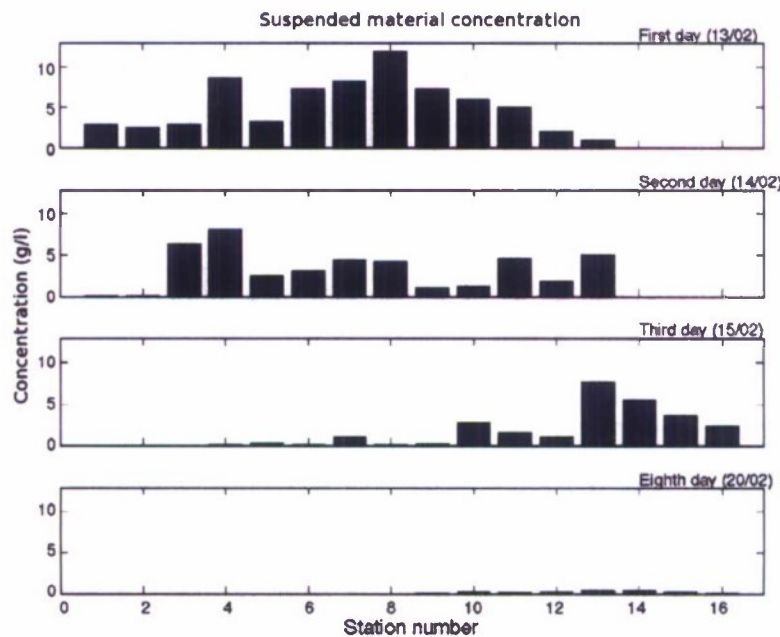

Fig. 8. Concentrations of suspended matter collected at the inner surf zone along the beach at the (a) first, (b) second, (c) third and (d) eighth days of the mud deposition. Station numbers are ordered from the most northern (Station 1) to the most southern one (Station 16).

(a) February 13 at 22:20 GMT **(b)** February 14 at 10:20 GMT **(c)** February 14 at 13:20 GMT **(d)** February 14 at 19:20 GMT
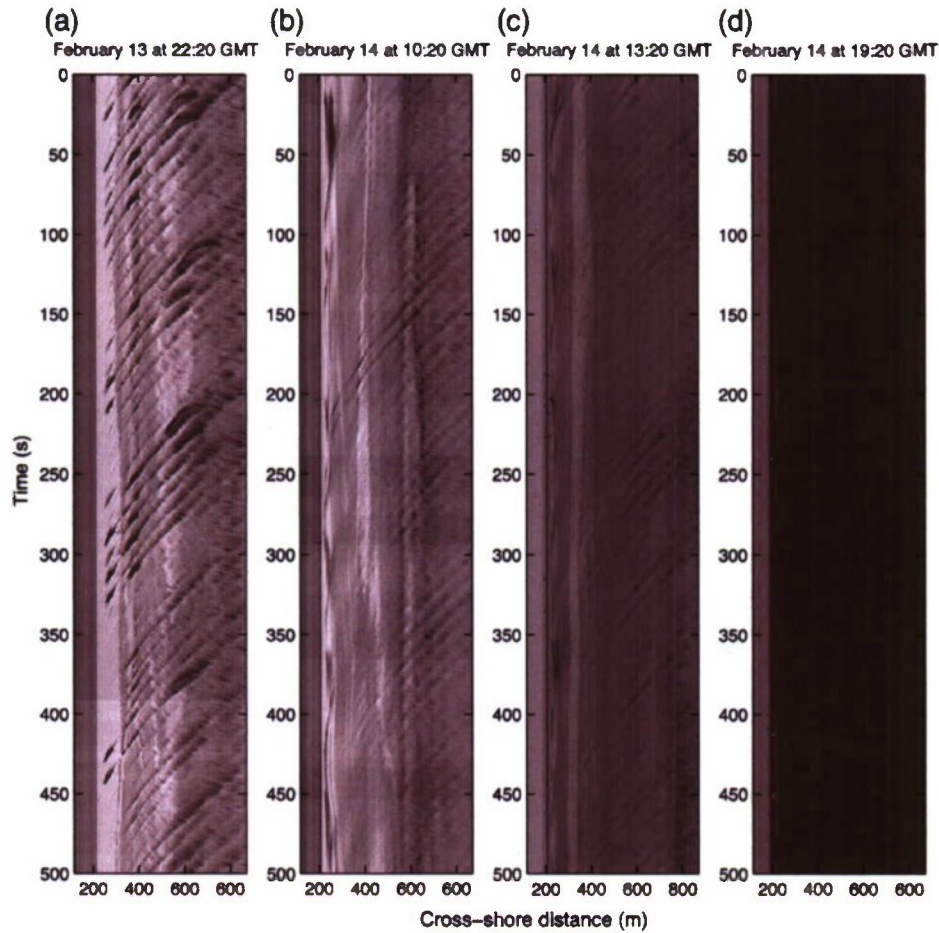
Cross–shore distance (m)

Fig. 9. Argus intensity timestack from (a) February 13 at 22:20 GMT and February 14 at (b) 10:20, (c) 13:20 and (d) 19:20 GMT.

so the wave-induced pressure extends from the water surface to the bottom (Dalrymple et al., 2008; Dean and Dalrymple, 1991). Gade (1958) was the first to study the effects of a nonrigid bottom on the surface waves in shallow water. This author employed a two-layer model, in which the water layer was assumed to be inviscid and the mud layer to be viscous. Gade's experiment showed that 80% of wave energy can be dissipated within a few wavelengths. The two-layer approach has also been the subject of other studies such as the work of Dalrymple and Liu (1978) and Ng (2000).

Despite the fact that wave attenuation is based on observed intensity data and spectra instead of wave height, some indicators provide evidence that the attenuation process is close to 100%. It should be highlighted here that although the model wave height data decrease from 5.5 m on February 13 to 4.5 m on February 14 (Fig. 3), significative energy still reached the beach. Taking a close look at Fig. 9 (stacks from Fig. 5), it is possible to notice that, as time passes, fewer waves (actually traces of wave crests) are detected. The absence of a spectral peak within the spectral range, attributed to surface water waves in Fig. 5f, indicates that no wave is propagating across the stack. Additionally Fig. 9 denotes the total absence of swash motions. In normal conditions, as the waves approach the shore, most of their energy is dissipated across the surf zone by wave breaking. However, a portion of the energy still gets to the shoreline, causing swash movements and its final dissipation and reflection upon the beach face. This leads to the occurrence of white foam up and down the

beach face, which results in an undulated behavior as can be seen in Fig. 4a. Such behavior is not displayed in Fig. 9, during the mud deposition event, indicating that almost 100% of the energy has been attenuated before reaching the shoreline.

Although real wave data were not available for Cassino beach during this period of time, the WW3 model data indicated that the swell did not end on February 14 (Fig. 3a); the predicted offshore wave height for this day was around 4 m. The peak direction presented in Fig. 3c also indicates that the waves were from southeast (130°), almost shore-normal. Visual time exposures (Fig. 10 right side) indicated that there were at least four active breaking lines in front of the Villa Moura Hotel on February 14, meaning there were waves that could be seen in the surf zone in areas without mud, which corroborates with the mentioned wave attenuation at the Argus station.

A few months after the deposition discussed here, in April 2008, Vinzon et al. (2008) measured density profiles and carried out wave measurements along a transect at the shoreface right in front of the Argus station, from the 18 m to 4.5 m depth contour. Their results indicated that mud still present over the shoreface could cause damping on the order of 40% of the wave height.

In addition to the decrease of wave traces in the intensity stacks, the optical signal of mud on the surface has been lost. As mentioned before, it was possible to detect the mud by video using its surface signal. This is corroborated by the integrated analysis of Figs. 6, 7,

(a) February 14 13:00 GMT

(b) February 14 13:00 GMT

(c) February 14 19:00 GMT

(d) February 14 19:00 GMT

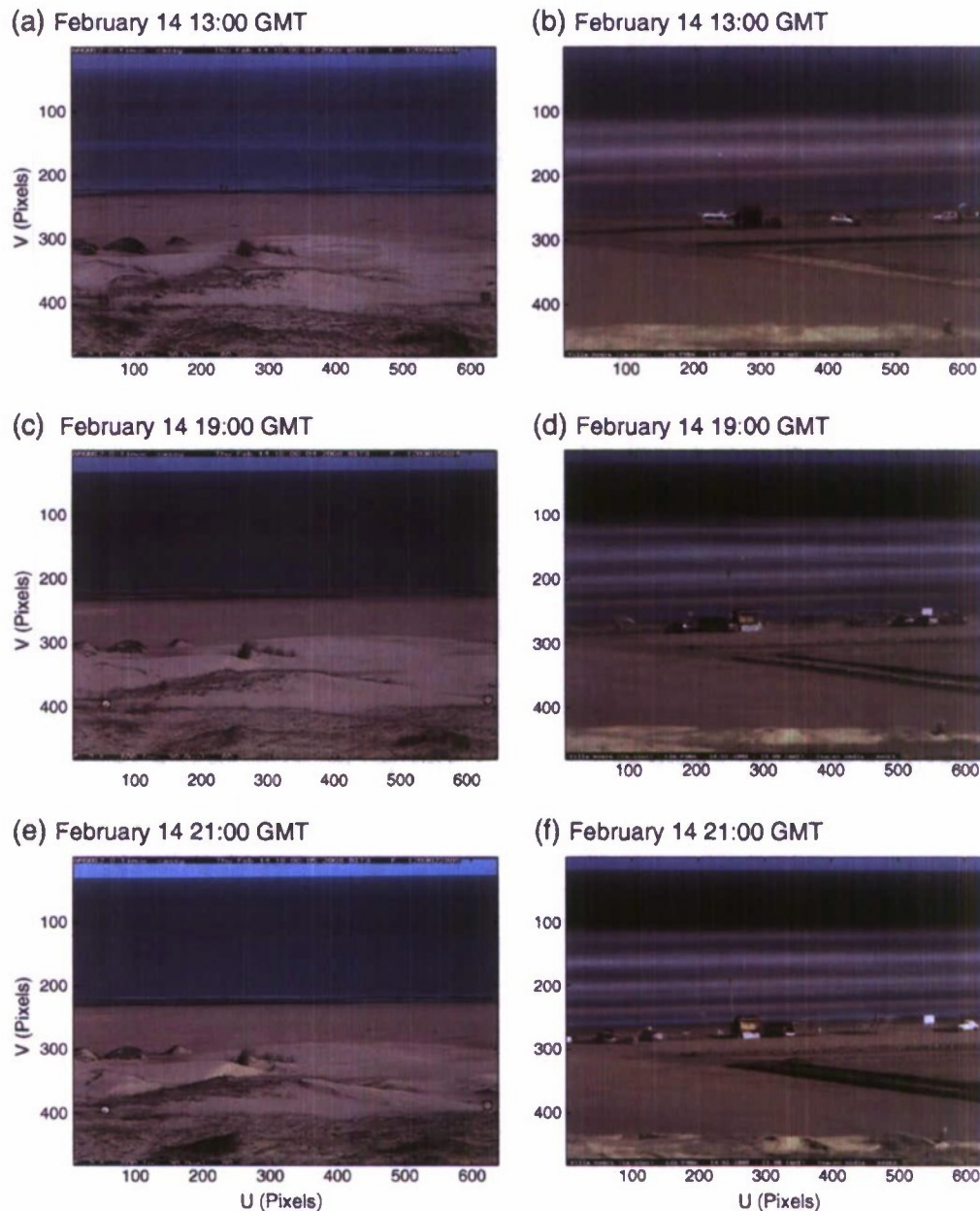## (e) February 14 21:00 GMT

(f) February 14 21:00 GMT

Fig. 10. Time exposure images of Cassino beach from the (left column) Argus station and (right column) from an equivalent system installed at the roof of the Villa Moura Hotel. The two stations are 3 km apart from each other. The images were captured simultaneously at (a and b) 13:00, (c and d) 19:00 and (e and f) 21:00 GMT.

8 and 9. The light gray tone on Fig. 9a located between x = 200 m and 300 m is the fluid mud shown in Fig. 8a, with suspended matter concentrations close to 6 g/l (Station 10). This fluid mud occupies the entire water column as seen in Fig. 7b. This same pattern found over the stack in Fig. 9a is lost as time passes (Fig. 9b through d), indicating the signal loss of mud on the surface, which in turn reduces the suspended matter concentration to 1.25 g/l (Fig. 8b).This signal loss is better illustrated by the profile at Fig. 6b, where the mud is lying over the sandy bottom forming a double layer system.

These results are corroborated by similar observations by Kineke et al. (2006) when studying resuspension and deposition patterns of cohesive sediments during cold front passages in the Gulf of Mexico. These authors showed that during pre-frontal conditions when wave

energy increases, sediment is resuspended, mixed and transported onshore. Post-front conditions also result in onshore transport and formation of a high concentration bottom layer increasing wave attenuation. The sequence described by Kineke et al. (2006) is similar to the processes occurring in the days before and after the deposition at Cassino beach. These authors state that the cold-front passages create a positive feedback mechanism where sediment is transported onshore by the waves (pre-front and post-front), that are attenuated through the interaction with the high suspended concentration and the unconsolidated bed.

Analysis of Figs. 5 and 6 indicates that this mechanism also occurs at Cassino beach and can be summarized using a conceptual scheme (Fig. 11). During the beginning of the process (first day), the mud
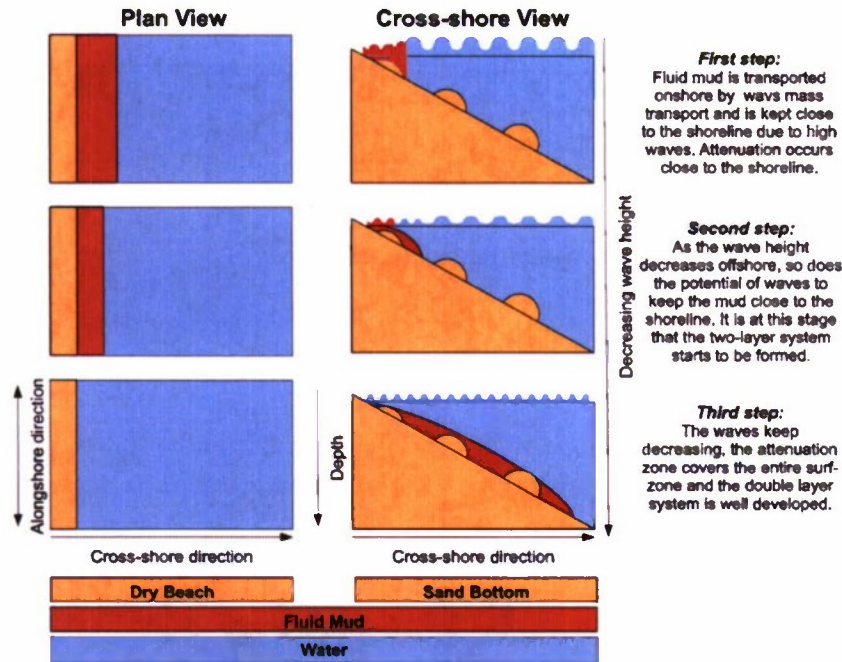
Fig. 11. Conceptual scheme of mud evolution after it has been transported towards the shoreline. As the wave height decreases the attenuation zone in the surf-zone increases. The left side of the figure shows a plan view and the right side a cross-shore view.

signal on the surface indicates the presence of fluid mud causing high wave attenuation at only the inner surf zone (first step). High waves in the outer surf-zone keep the mud close to the shoreline due to wave mass transport. As the wave height decreases (second day), the energy to maintain the mud at the inner surf zone also decreases and the deposit starts to settle and migrate offshore as a gravity driven flow creating a double layer system (second step). At this stage, as shown in Fig. 5 (from d to f) the attenuation process occurs in a scale of 100 m (third step).

An issue that still remains to be solved is whether the mud migrates as a massive block or as patches of fluid mud. Some peculiar low frequency oscillations in the most landward intensity patterns (Fig. 9a and b) suggest that mud is migrating as patches in time intervals as short as a few minutes. However, to clarify this aspect, a continuous collection of suspended matter across the surf zone or the deployment of an array of optical backscatter sensors is needed.

7. Summary and conclusion

The Argus video-based system at Cassino demonstrated that remote detection of fluid mud is possible as well as quantification of its effect on the nearshore dynamics. The combination of beach profiles, measurements of suspended matter concentration and intensity timestacks allowed the analysis of the short-term evolution of the mud depositional processes and its effect on the surf-zone. In short, after resuspension, mud undergoes onshore transport and is kept in the entire water column by wave energy from the outer surf-zone. As the wave energy decreases, the mud settles and migrates offshore as a density-driven flow, generating a two layer system, in which a viscous mud layer is underneath the water column and overlies a sandy bottom. This system enhances wave attenuation through a strong positive feedback mechanism which damps nearly 100% of the initial wave energy. This two-layer system coincides with the loss of the surface wave signal, which in turn results in the attenuation of the incident peak period band measured from frequency–space plots.

While not accurately comparable to conventional field survey techniques, video-based methods are less expensive, can be sampled more frequently, for longer periods of time and require simple logistics. Due to the unpredictable occurrence of the mud deposition process on Cassino beach, such characteristics are essential, as demonstrated during the field study of coastal dynamics on a muddy beach in 2005 (Holland et al., 2009). This unpredictability makes the deployment of fixed equipment on the surf-zone very exhaustive and expensive, thus, encouraging the use of remote sensing video-techniques.

References

Augustinus, P., Hazelhoff, L., Kroon, A., 1989. The chenier coast of Suriname: modern and geological development. Marine Geology 90, 269–281.
Bowen, A.J., Inman, D.L., Simmons, V.P., 1968. Wave 'set-down' and set-up. Journal of Geophysical Research 73, 2569–2577.
Calliari, L., Tozzi, H., Klein, A., 1998. Beach morphology and coastline erosion associated with storm surges in Southern Brazil—Rio Grande to Chuí, RS. Land and Ocean Interaction in Coastal Zone (LOICZ) Meeting, São Paulo, SP, Brazil, pp. 231–247.
Calliari, L.J., Speranski, N.S., Torronteguy, M., Oliveira, M.B., 2001. The mud banks of Cassino Beach, Southern Brazil: characteristics, processes and effects. Journal of Coastal Research 34, 318–325.

Calliari, L.J., Holland, K.T., Pereira, P.S., Guedes, R.M.C., Santo, R., 2007. The influence of mud on the inner shelf, shoreface, beach and surf zone morphodynamics—Cassino, Southern Brazil. Coastal Sediments'07, New Orleans, MS, pp. 1–11.

Calliari, L., Winterwerp, J., Fernandes, E., Vinzon, S., Cuchiara, D., Holland, K., Sperle, M., 2009. Fine grain sediment transport and deposition in the Patos Lagoon–Cassino beach sedimentary system. Continental Shelf Research 29, S1S–S29.

Dalrymple, R., Liu, P., 1978. Waves over soft muds: a two-layer fluid model. Journal of Physical Oceanography 8, 1121–1131.

Dalrymple, R., Nouri, Y., Sabouri-Shargh, Z., 2008. Water waves propagating over mud. International Conference on Coastal Engineering, Hamburg, Germany, pp. 314–323.

Dean, R., Dalrymple, R., 1991. Water Wave Mechanics for Engineers and Scientists. World Scientific, Singapore.

Gade, H., 1958. Effects of a nonrigid, impermeable bottom on plane surface waves in shallow water. Journal of Marine Research 16 1-61-82.

Holland, K., Elmore, P., 2008. A review of heterogeneous sediments in coastal environments. Earth Science Reviews 89, 116–134.

Holland, K., Holman, R., Lippmann, T., Stanley, J., Plant, N., 1997. Practical use of video imagery in nearshore oceanographic field studies. IEEE Journal of Oceanic Engineering 22, 81–92.

Holland, K., Vinzon, S., Calliari, L.J., 2009. A field study of coastal dynamics on a muddy coast offshore of Cassino beach, Brazil. Continental Shelf Research 29, S03–S14.

Holman, R., 1995. Nearshore processes. Reviews of Geophysics 33, 1237–1247.

Holman, R., Stanley, J., 2007. The history and technical capabilities of Argus. Coastal Engineering 54, 477–491.

Kineke, G., Higgins, E., Hart, K., Velasco, D., 2006. Fine-sediment transport associated with cold-front passages on the shallow shelf, Gulf of Mexico. Continental Shelf Research 26, 2073–2091.

Marques, W., 2009. Estudo da dinâmica da pluma costeira da Lagoa dos Patos. Phd thesis. Federal University of Rio Grande.

Marques, W., Fernandes, E., Monteiro, I., Möller, O., 2009. Numerical modeling of the Patos Lagoon coastal plume, Brazil. Continental Shelf Research 29, S56–S71.

Marques, W.C., Fernandes, E.H.L., Moraes, B.C., Möller, O.O., Malcherek, A., 2010. Dynamics of the Patos Lagoon coastal plume and its contribution to the deposition pattern of the southern Brazilian inner shelf. Journal of Geophysical Research 115, C1004S. doi:10.1029/2010JC006190.

Mathew, J., Baba, M., Kurian, N., 1995. Mudbanks of the southwest coast of India 1. Wave Characteristics. Journal of Coastal Research 11, 168–178.

Melo, E., Hammes, G., Franco, D., Romeu, M., 2008. Aferição de desempenho do modelo WW3 em Santa Catarina. Anais do III Seminario e Workshop em Engenharia Oceanica (SEMENGO), Rio Grande, RS, Brazil, p. 20.

Möller, O., Castaing, P., Salomon, J., Lazure, P., 2001. The influence of local and non-local forcing effects on the subtidal circulation of Patos Lagoon. Estuaries 24, 297–311.

Ng, C., 2000. Water waves over a muddy bed: a two-layer Stokes boundary layer model. Coastal Engineering 40, 221–242.

Strauch, J., 1998. Um ano de monitoramento de ondas em Rio Grande. Final Proceedings of the XI National Week of Oceanography, Oceanography and their interfaces. Federal University of Rio Grande—FURG, Rio Grande, Rio Grande do Sul, Brazil.

Tomazelli, L., 1993. O regime dos ventos e a taxa de migração das dunas eólicas costeiras do Rio Grande do Sul, Brasil. Pesquisas em Geociências 20, 18–26.

Vinzon, S., Meirelles, S., Leão, T., 2008. Wave generated lutoclines offshore of Cassino Beach, Brazil. PECS 2008: Physics of Estuaries and Coastal Seas, Liverpool, UK, pp. 369–372.

Vinzon, S., de Boer, G., Winterwerp, J., Nogueira, R., 2009. Mud deposit formation on the open coast of the larger Patos Lagoon–Cassino Beach system. Continental Shelf Research 29, S72–588.

Wells, J., 1983. Dynamics of coastal fluid muds in low, moderate and high tide range environments. Canadian Journal of Fisheries and Aquatic Sciences 40, 130–142.

Wells, J., Coleman, J., 1977. Nearshore suspended sediment variations, central Surinam coast. Marine Geology 24, 47–54.

Wells, J., Coleman, J., 1981. Physical processes and fine-grained sediment dynamics coast of Surinam, South America. Journal of Sedimentary Petrology 51, 1053–1068.

Wells, J., Coleman, J., Wiseman, W.J., 1979. Suspension and transportation of fluid mud by solitary-like waves. Proceedings of the 16th Coastal. Engineering Conference. ASCE, Hamburg, Germany, pp. 1932–1951.

Winterwerp, J., Graaff, R., Groeneweg, J., Luijendijk, A., 2007. Modelling of wave damping at Guyana mud coast. Coastal Engineering 54, 249–261.